Programmable immune activating electrospun fibers for skin regeneration

Lu Chen [a,1], Liucheng Zhang [a,1], Hongbo Zhang [b,d,1], Xiaoming Sun [a], Dan Liu [c], Jianming Zhang [c], Yuguang Zhang [****,a], Liying Cheng [a,***], Hélder A. Santos [e,f,**], Wenguo Cui [b,*]

[a] Department of Plastic and Reconstructive Surgery, Shanghai Ninth People's Hospital, Shanghai Jiao Tong University School of Medicine, 639 Zhi Zao Ju Road, Shanghai 200011, PR China
[b] Shanghai Key Laboratory for Prevention and Treatment of Bone and Joint Diseases, Shanghai Institute of Traumatology and Orthopaedics, Ruijin Hospital, Shanghai Jiao Tong University School of Medicine, 197 Ruijin 2nd Road, Shanghai 200025, PR China
[c] National Research Center for Translational Medicine, Ruijin Hospital, Shanghai JiaoTong University School of Medicine, 197 Ruijin 2nd Road, Shanghai 200025, PR China
[d] Department of Pharmaceutical Sciences Laboratory and Turku Center for Biotechnology, Åbo Akademi University, Turku FI-20520, Finland
[e] Drug Research Program, Division of Pharmaceutical Chemistry and Technology, Faculty of Pharmacy, University of Helsinki, Helsinki FI-00014, Finland
[f] Helsinki Institute of Life Science (HiLIFE), University of Helsinki, Helsinki FI-00014, Finland

ARTICLE INFO

ABSTRACT

Immune cells play a crucial regulatory role in inflammatory phase and proliferative phase during skin healing. How to programmatically activate sequential immune responses is the key for scarless skin regeneration. In this study, an "Inner-Outer" IL-10-loaded electrospun fiber with cascade release behavior was constructed. During the inflammatory phase, the electrospun fiber released a lower concentration of IL-10 within the wound, inhibiting excessive recruitment of inflammatory cells and polarizing macrophages into anti-inflammatory phenotype "M2c" to suppress excessive inflammation response. During the proliferative phase, a higher concentration of IL-10 released by the fiber and the anti-fibrotic cytokines secreted by polarized "M2c" directly acted on dermal fibroblasts to simultaneously inhibit extracellular matrix overdeposition and promote fibroblast migration. The "Inner-Outer" IL-10-loaded electrospun fiber programmatically activated the sequential immune responses during wound healing and led to scarless skin regeneration, which is a promising immunomodulatory biomaterial with great potential for promoting complete tissue regeneration.

1. Introduction

Scar formation characterized by excessive extracellular matrix (ECM) deposition is a common consequence of wound healing, and it currently has no ideal therapy in clinic [1]. Several studies have shown that the inflammatory and proliferative phases in the sequential wound healing process play a decisive role in the outcomes of wound healing [2–4]. The inflammatory phase begins immediately after the wound forms and generally lasts for 3–5 days [5]. In this phase, inflammatory cells, including macrophages, are recruited to the wound to remove local

pathogenic microorganisms [6]. The proliferative phase occurs after the inflammatory phase and ends until the epithelialization is complete. During this phase, fibroblasts proliferate and migrate by various pro-repair factors' regulation, and produce a large amount of ECM to fill the tissue defect. Over-reactive inflammatory response during the inflammatory phase or excessive deposition of ECM in the proliferation phase will cause abnormal scar formation. Therefore, the sequential immunoregulation during the inflammatory and proliferative phases is the key to promote scarless skin regeneration.

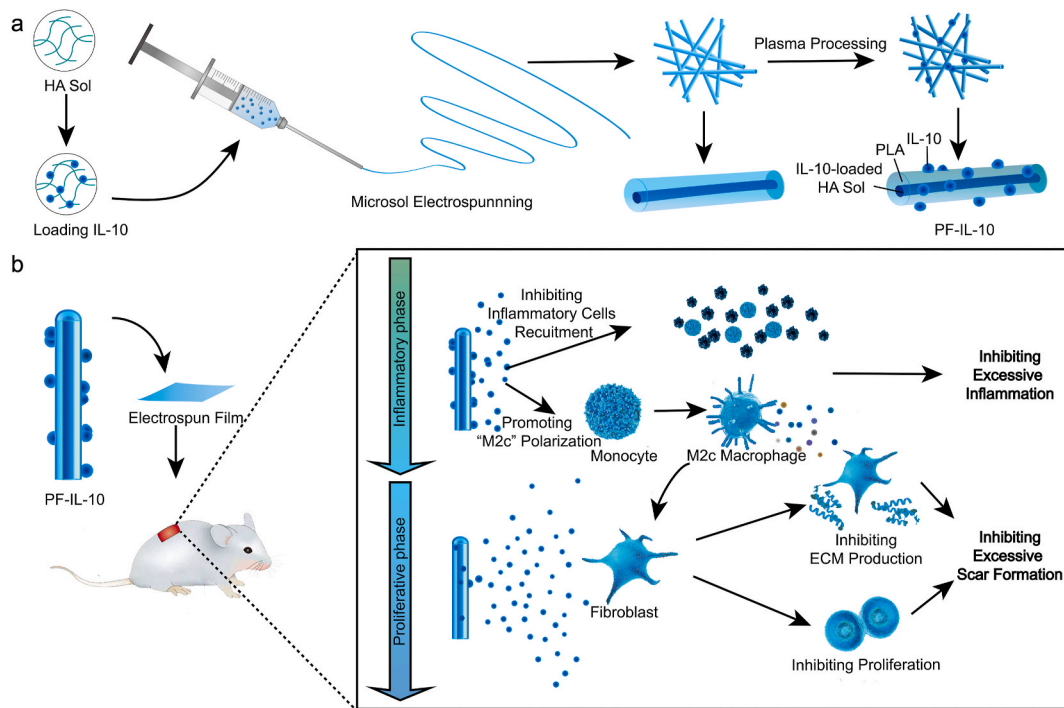The immune response regulation network mediated by various

Fig. 1. Schematic of the "Inner-Outer" IL-10-loaded electrospun fiber for scarless skin regeneration. (a) Diagram of constructing "Inner-Outer" IL-10-loaded electrospun fibrous membrane with microsol-electrospinning technology and plasma treatment procedure. (b) Illustration of the programmable immune activation effect of the "Inner-Outer" IL-10-loaded electrospun fiber during the inflammatory phase and the proliferative phase of wound healing process.

immune factors and immune cells directly affects the outcome of tissue regeneration. IL-10 is often considered to be the dominant anti-inflammatory player in wound healing [7]. Properly increasing the concentration of local IL-10 during the inflammatory phase reduces the expression of proinflammatory cytokines and inhibits excessive recruitment of immune cells, thus suppressing the hyperinflammatory response stimulated by injury [8]. During the proliferative phase, IL-10 of a high concentration directly acts on fibroblasts to inhibit the production of ECM components [8,9]. In addition, recent studies have demonstrated that IL-10 in damaged tissues can also polarize monocyte recruited into "M2c" macrophages [10]. This subtype of M2 macrophages is characterized by high expression of anti-inflammatory mediators and anti-fibrotic factors, regulating inflammatory response and matrix deposition, and leading to a microenvironment conducive for tissue regeneration [11–13]. Considering the effect of IL-10 on polarizing monocytes into "M2c" and concentration-dependent influence on macrophages recruitment and ECM production, constructing a programmable immune regulatory network dominated by IL-10 and "M2c" to precisely regulate the immune response during wound healing is a reliable strategy.

Due to the topographical similarity to the native ECM, good tissue compatibility, and high plasticity of morphology, electrospun membranes are often used as substitutes in tissue engineering [14–16]. In recent years, with continuous exploration of the drug-loading fibers and in-depth understanding of the regulatory mechanism of cytokines, cytokine-loaded electrospun fiber has extensively been studied in the field of tissue regeneration [17]. However, previous studies have neglected the changing phased immunologic characteristics of tissue healing, leading to limited pro-regenerative effects. Therefore, how to develop a cytokine-loaded electrospun fiber with cascade-releasing characteristics to coordinate the sequential and overlapping phases of wound healing and programmatically activate the phased immune response during the regeneration process is still a critical challenge to be solved.

In this study, microsol-electrospinning technology and plasma

treatment procedure was used to construct the "Inner-Outer" IL-10-loaded electrospun fiber with core-shell structure (Fig. 1a). Through microsol electrospinning technology, hyaluronic acid (HA) nanoparticles loaded with IL-10 formed the "core" of fiber, causing a delayed release effect. While IL-10 grafted on the plasma treated surface was quickly released by diffusion. By controlling the amount of cytokines loaded inside and outside, a concentration controlled cascade release was achieved (Fig. 1b). The local concentration of IL-10 released by the "Inner-Outer" IL-10-loaded electrospun fiber was relatively low in the first 5 days, which avoided over suppressing macrophages recruitment and meanwhile effectively polarized the macrophages into "M2c", thus inhibiting excessive inflammation during the inflammatory phase. From day 6 to day 15, the local IL-10 of a higher concentration and the pro-repair factors released by "M2c" acted on fibroblasts simultaneously during the proliferative phase, which significantly inhibited fibroblast over-proliferation and ECM excessive deposition, thus scarless skin regeneration achieving. The "Inner-Outer" IL-10-loaded electrospun fiber with cascade release behavior is in close coordination with wound healing process, which programmatically activates the sequential immune responses during skin regeneration, showing tremendous pro-regenerative potential.

2. Materials and methods

2.1. Materials

Polylactidic acid (PLA) (Mw = 100 kDa, Mw/Mn = 1.85) was purchased from Jinan Daigang Co. (China). Fermentation-derived hyaluronic acid (HA) (sodium salt, Mw = 0.5 MDa) was purchased from Yuancheng Technology Co. (Wuhan, China) and used without further purification. Recombinant Human IL-10 (h-IL-10) and Recombinant Murine IL-10 (m-IL-10) were purchased from PeproTech (USA). Hoechst 33,342 Staining Solution for Live Cells was purchased from Beyotime Biotechnology (Shanghai, China). RPMI 1640 medium, Dulbecco's modified Eagle's medium (DMEM), fetal bovine serum (FBS), 0.25%

trypsin-EDTA (1 ×), Penicillin-Streptomycin liquid, phosphate-buffered saline (PBS, pH 7.4) were purchased from Gibco (USA). Phorbol 12-myristate 13-acetate (PMA) was purchased from Sigma-Aldrich (USA). All other reagents were obtained from Dai Xuan Biological Technology Co. LTD (China) unless otherwise indicated.

2.2. Fibroblast culture

In order to obtain the fibroblasts with the ability to produce a large amount of ECM, we collected hypertrophic scar specimens from the patients (1 male and 2 females) of Plastic and Reconstructive Surgery Department of Shanghai Ninth People's Hospital. The patients provided their written, informed consents. The rinsed tissues were sectioned into small pieces and incubated in 0.3% NB4 collagenase (SERVA, Heidelberg, Germany) at 37 °C for 4 h. The isolated fibroblasts were subsequently cultured and used in this experiment at passage 3.

2.3. Production of electrospun membrane

PLA electrospun fiber without IL-10 loaded (PF), electrospun fibers loaded IL-10 inside, and electrospun fibers loaded IL-10 outside were constructed to investigate the release characteristics of IL-10 loaded electrospun fibers.

For preparing PF, 1 mg HA was dissolved in 1 mL distilled water. After ultrasonic emulsification, HA-sol nanoparticles were formed (Fig. S1). 200 μL HA-sol nanoparticles were dispersed in a solvent mixture containing 6.42 mL dichloromethane (DCM), 0.01 g Span-80, and 1 g PLA. After 1 day of mixture, the electrospinning solution was put into a 10 mL syringe with a metal needle. The inner diameter of the metal needle was 0.9 mm. The flow rate of the solution was 80 μL/min and was controlled by a microinject pump (Lange Medical Instrument Co., Baoding, Hebei, China). An electrically grounded aluminum foil was used to collect electrospun fibers. With a distance of about 15 cm to the foil, the end of needle was attached with a metal clip which was connected to the DC high-voltage power supply (Tianjin Dongwen High-voltage Power Supply Co., China). The voltage was ranging from 15 to 25 kV (Fig. S2a). For preparing electrospun fibers loaded IL-10 inside, 1 mg HA was dissolved in 1 mL of either 2.5 μg/mL, 5 μg/mL, or 10 μg/mL of recombinant human IL-10 (h-IL-10, PeproTech, USA), respectively; and used to make electrospun fiber as above mentioned. For preparing electrospun fibers loaded IL-10 outside, the fibers with HA-sol nanoparticles loaded inside were surface modified by a plasma cleaner (PDC-MG, ING Heng Company, Changzhou, China). Oxygen plasma treatment was done at the voltage around 600–800 V for 3 min. Then the treated scaffolds of 100 mg were immersed into 1 mL of IL-10 solution at a concentration of 250 ng/mL, 500 ng/mL, and 1000 ng/mL for 24 h respectively to construct electrospun fibers loaded different amount of IL-10 outside. After that, the IL-10-surface-coated scaffolds were rinsed with PBS for 5 times and dried by a freeze dryer (Wuxi Voshin Instruments Manufacturing Co. LTD), according to the practical guideline. The amount of IL-10 fixed on the surface of electrospun fibers is the amount of IL-10 in the initial soaking solution minus the amount of IL-10 remaining in the solution and the amount of IL-10 in the washing solution, which were determined by an enzyme linked immunosorbent assay (ELISA).

2.4. IL-10 of different concentration on macrophages and fibroblasts

In order to determine the effects of IL-10 of different concentrations on cell viability and macrophage recruitment, we conducted *in vivo* and *in vitro* experiments. For macrophages, on the one hand, we explored the cytotoxicity of IL-10 to macrophages by culturing which with h-IL-10 of different concentration (0 ng/mL, 10 ng/mL, 50 ng/mL, 100 ng/mL, 200 ng/mL, and 500 ng/mL); on the other hand, different concentrations of m-IL-10 were injected subcutaneously immediately after wound formation. Cell Counting Kit-8 (CCK-8) Detection Kit (Dojindo

Molecular Technologies, Tokyo, Japan) and Cytotoxicity Detection Kit (Sigma-Aldrich, USA) were used to detected the *in vitro* cell viability of IL-10 stimulated macrophage [18]. Hematoxylin & Eosin (H&E) staining and immunohistochemistry (IHC) staining (Servicebio, Wuhan, China) were used to assess the recruitment and polarization of macrophages on day 3. Similarly, the viability of fibroblasts cultured with h-IL-10 of different concentration was determined by CCK-8 Detection Kit and Cytotoxicity Detection Kit.

2.5. In vivo release behavior study

The factors that affect the local concentration of IL-10 released are mainly determined by the release characteristic of electrospun fiber, local blood circulation, cytokine clearance rate, and the volume of tissue fluid, which are difficult to quantify directly. In order to clarify the concentration relationship between the release concentration *in vivo* and *in vitro*, and minimize the result deviation caused by measurement, the fiber loaded with 10 μg/mL of IL-10-HA-sol inside, the fiber grafted with 1000 ng/mL of IL-10 outside, and the fiber loaded with 10 μg/mL of IL-10-HA-sol inside and grafted with 1000 ng/mL outside simultaneously were evaluated. In brief, the fiber membrane was covered the full-thickness excisional wounds of 1.5 cm × 1.5 cm made on the back of C57BL/6 mice (20–25 g, 8-10-week age, purchased from the Experimental Animal Center of Shanghai Ninth People's Hospital). The tissue fluid of local skin was collected and measured by ELISA, respectively, on day 3, day 7, day 15. The method of obtaining tissue fluid is as previous studies [19,20].

2.6. In vitro release behavior study

To study the release behavior of the scaffolds, 100 mg of fibrous membranes of the electrospun fibers loaded with different concentrations of IL-10 inside and/or outside were respectively immersed in 3 mL of PBS, which was placed in a thermostatic water bath at 37 °C. 100 μL releasing buffer was collected from each group daily for 15 days (n = 3). After that, we added 100 μL PBS to replace the volume of the releasing buffer took out. The concentration of the releasing buffer of h-IL-10-loaded fibers was determined by ELISA kit (Boster Biological Technology co. ltd, California, USA), according to the manufacturer's protocol. The amount of IL-10 was determined from a calibration curve based on known concentrations of IL-10.

After that, with known the release behavior of "Inner" IL-10 loaded fiber, "Outer" IL-10 loaded fiber, and "Inner-outer" IL-10 loaded fiber of different concentration combinations, and the *in vivo* and *in vitro* release concentration of the same fibrous membrane, we assigned the fiber loaded with 10 μg/mL of IL-10-HA-sol inside as In-IL-10@PF (Fig. S2b) and the plasma treated fiber immersed into 500 ng/mL of IL-10 solution as PF@Ex-IL-10 (Fig. S2c). Also, the 10 μg/mL IL-10-HA-sol loaded PLA electrospun fiber with 500 ng/mL IL-10 grafted outside was assigned as PF-IL-10 for further investigation (Fig. 1a), regarding the phased process of wound healing.

2.7. Morphological characterization of fibers

For morphological characterization, various fibrous morphologies were measured by scanning electron microscope (SEM, Hitachi, S-4800, Japan) at an accelerating voltage of 10 kV and transmission electron microscope (TEM, Hitachi, HT7700, Japan) at a voltage of 120 kV. A layer of platinum was sprayed over the sample surfaces before SEM observation. The average diameters of both the external structure and the inner structure were analyzed by measuring a total of 100 random fibers with Image J software (National Institutes of Health, Bethesda, MD). To visualize the IL-10 distribution, we labeled h-IL-10 with fluorescein isothiocyanate (FITC). After dialyzed to remove any residual FITC, the labeled h-IL-10 was encapsulated into PLA-microsol fibers or coated on the surface of fibers, as above-mentioned. Electrospun fibers

with fitc-h-IL-10 encapsulated or coated on the surface were examined with confocal laser scanning microscope (CLSM, Leica TCS SP2, Germany). The Excitation and emission wavelengths were set at 488 and 535 nm, respectively.

2.8. Biocompatibility evaluation

Fibroblasts were used to evaluate the biocompatibility of fibrous scaffolds. Before cell seeding, all the fibrous mats were sterilized by electron-beam irradiation using linear accelerator (PreciseTM, Elekta, Crawley, UK) with a total dose of 80 cGy. After that, the fibroblasts at a density of 2×10^4/mL were seeded onto the pre-soaked fibrous mats (n = 6). The cell seeded mats were incubated at 37 °C for 3 days. On day 1 and day 3, the mats for fibroblast growth were rinsed for 3 times respectively to remove the dead suspended cells. After that, the fibroblasts seeded were stained by Hoechst 33,342 (Beyotime, China) for adherent living cell count assay. Further, to observe the morphologies of fibroblasts seeded on the membranes, the fibrous mats were harvested on day 3 after seeding and dehydrated using graded ethanol before SEM observation.

2.9. Releasing buffer collection for fibroblast culture

500 mg fibers of PF group and of PF-IL-10 group were respectively immersed into 15 mL of DMEM for 15 days, which simulated the proportional release of IL-10 and material degradation products during the proliferation phase of wound healing [21–23]. The releasing buffer collected on day 15 was added with 10% of FBS and 1% penicillin-streptomycin liquid, which was used as culture medium of PF group and PF-IL-10 group. DMEM mixed with 10% of FBS and 1% penicillin-streptomycin liquid was used as control.

2.10. Fibroblast culture with releasing buffer

The fibroblasts obtained by the method above-mentioned were cultured at 37 °C with 95% relative humidity and 5% CO_2 partial pressure (n = 6). The morphologies of fibroblasts were observed at 0-h and 24-h. Compared with the control group, the effect of different group of releasing buffer on the proliferation and apoptosis of fibroblasts was detected by a CCK-8 kit, a Dead Cell Apoptosis Kit with Annexin V Alexa Fluor® 488 and propidium iodide (PI) (Gibco, USA), and a Cytotoxicity Detection Kit, according to the manufacturer's protocols.

2.11. Scratch migration experiment

Fibroblasts were seeded in 6-well culture plates at a density of 5×10^5 cells per well (n = 6). A confluent monolayer of cell was formed after overnight culture. Gaps without cell attachment were scratched with a 200-μL pipette tip. Images were collected at the same position of the plate at 0-h, 6-h, 12-h and 24-h. Image J software was used to quantify the migrated area.

2.12. PCR analysis

PCR was performed on RNA to detect the expression of scar related genes, including Col I, Col III, α-SMA, and TGF-β1 (n = 6). In brief, total RNAs of cultured cells treated with releasing buffer for 24 h were extracted using RNA-isolation kit (Takara, Japan). The purity of RNA obtained was evaluated by the calculated A260/A280 (1.9–2.0). The primer pairs (human) used for gene amplification from the cDNA template were as follows: Col I: forward 5′-GAGGGCAA-CAGCAGGTTCACTTA-3′ and reverse 5′-TCAGCACCACCGATGTCCA-3′; Col III: forward 5′-CCACGGAAACACTGGTGGAC-3′ and reverse 5′-GCCAGCTGCACATCAAGGAC-3′; α-SMA: forward 5′-GACAATGGCTCTGGGCTCTGTAA-3′ and reverse 5′-TGTGCTTCGTCACCCACGTA-3′; TGF-β1: forward 5′-TGGTGGAAACCCACAACGAA-3′ and reverse 5′-GAGCAA-CACGGGTTCAGGA-3′; and glyceraldehyde 3-phosphate dehydrogenase (GAPDH): forward 5′-GCACCGTCAAGCTGAGAAC-3′ and reverse 5′-TGGTGAAGACGCCAGTGGA-3′. The relative expression levels of the corresponding target genes' transcripts were normalized against the expression level of the housekeeping gene GAPDH.

2.13. Western blotting analysis

Western blotting analysis was performed with the adherent cell treated with releasing buffer for 24 h. Briefly, equal amounts of protein in the cell lysates were subjected to electrophoresis on 7% of poly-acrylamide gel electrophoresis (SDS-PAGE) gel at 110 V, followed by transferring to poly (vinylidene fluoride) (PVDF) membranes. After blocked with 5% of albumin from bovine serum (BSA) for 2 h at room temperature, the membranes were incubated with antibodies of Col I (Rabbit, 1:3000; Abcam, Cambridge, UK), Col III (Rabbit, 1:1000; Abcam, Cambridge, UK), α-SMA (Rabbit, 1:1000; Abcam, Cambridge, UK), TGF-β1(Rabbit, 1:1000; Abcam, Cambridge, UK), and β-actin antibodies (Goat, 1:500; Santa Cruz Biotechnology, Inc., Dallas, TX, USA). After being washed four times with Tris-Buffered Saline Tween-20 (TBST), the immunoreactive traces were detected by an enhanced chemiluminescence (ECL) detection kit (Amersham Biosciences, Chalfont St. Giles, UK). The intensity of protein expression on the membranes was analyzed by Image J software.

2.14. Polarization and characterization of macrophages

Human myeloid leukemia mononuclear cells (THP-1 monocyte) (cat. no. TIB-202) was purchased from the Type Culture Collection of the Chinese Academy of Sciences (Shanghai, China), and was propagated *in vitro* with RPMI-1640 medium (Gibco, USA) containing 10% of FBS. To differentiate the THP-1 cell into macrophages, the undifferentiated THP-1 cells were seeded at 1×10^6 cells/mL and cultured in RPMI-1640 supplemented with 200 nM of PMA and 10% of FBS in a 5% CO_2 incubator at 37 °C for 3 days. Subsequently, the releasing buffers of PF electrospun membranes and PF-IL-10 electrospun membranes was collected on day 3, which simulated the proportional release of IL-10 and material degradation products during the inflammation phase of wound healing [21–23]. The releasing buffers were added with 10% of FBS, 100 mg/mL of streptomycin, and 100 units/mL of penicillin, which were used to polarize PF-induced macrophages and PF-IL-10-induced macrophages separately. The cell culture supernatant/conditioned medium of THP-1 cell, PMA-treated THP-1 cell, PF-induced macrophage, and PF-IL-10-induced macrophage were collected for further experiment. To evaluate the expression of CD163-APC, CD206-PE, TLR1-PE, and TLR8-PE in THP-1 cells, PMA-treated THP-1 cells, PF-stimulated macrophages, and PF-IL-10-stimulated macrophages, cells were incubated with antibodies for human CD163-APC (Invitrogen, Carlsbad, California, USA), CD206-PE (eBioscience, San Diego, CA, USA), TLR1-PE (eBioscience, San Diego, CA, USA), or TLR8-PE (Invitrogen, Carlsbad, California, USA) for 30 min at room temperature. Subsequently, cells were washed twice with PBS, and then analyzed by flow cytometry (FACSAria I; BD Biosciences, Oxford, UK) (n = 6). Kaluza software (version 1.2; Beckman Coulter, USA) was used to analyze the data. The production of IL-10 and TGF-β1 by macrophage was measured by an enhanced ELISA kit (Boster Biological Technology Co., California, USA), according to manufacturer's instruction (n = 6). Because of the low level of IL-10 in the conditioned medium of stimulated macrophages and monocytes, the standard curve was specially extended to a lower range reliably by further diluting the IL-10 standard.

2.15. Fibroblasts cultured with conditioned medium of monocytes/ macrophages

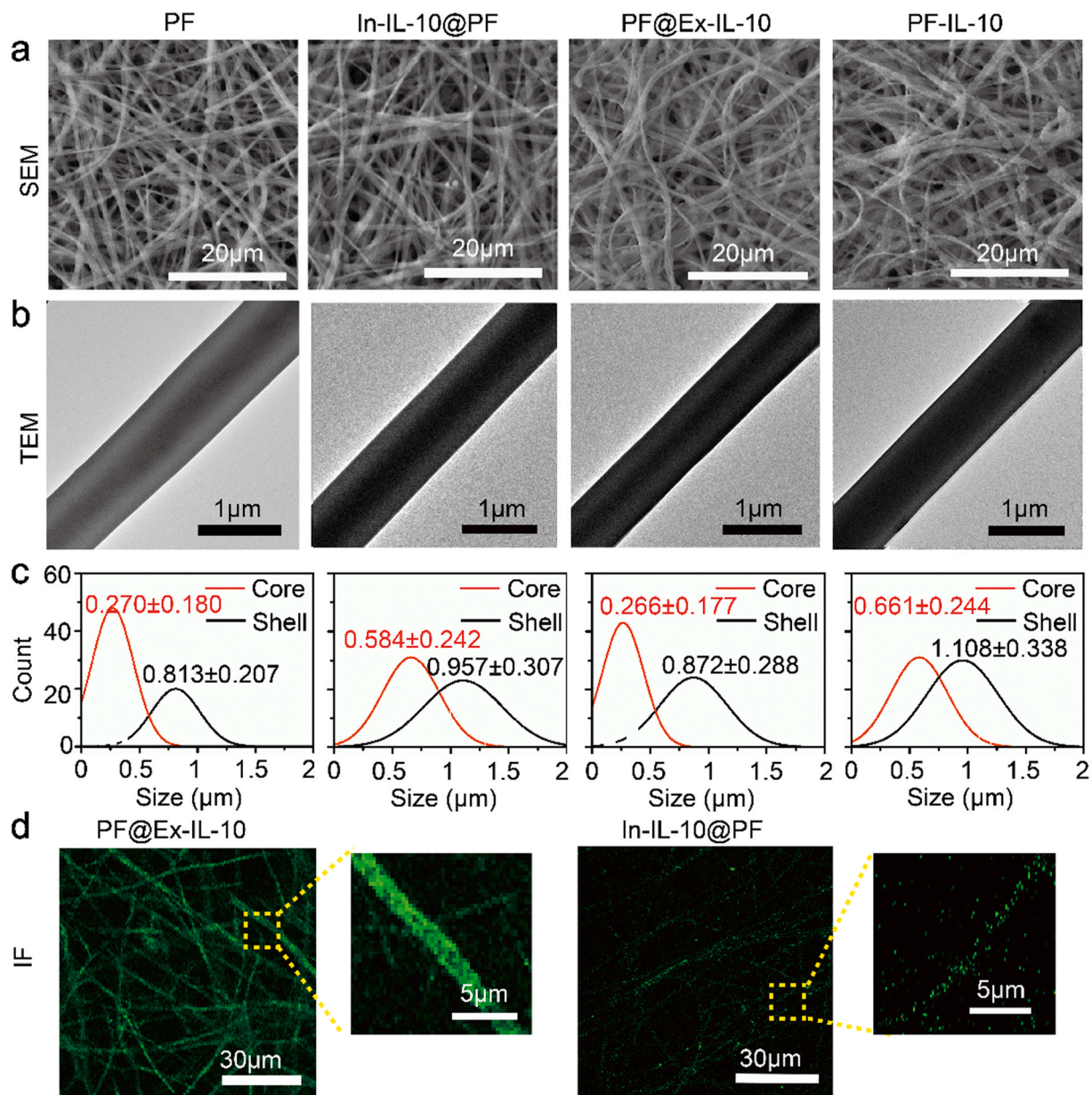The observation of morphology, proliferation and apoptosis of

Fig. 2. Morphology of different membranes. (a) SEM micrographs and (b) TEM images of PF, In-IL-10@PF, PF@Ex-IL-10, and PF-IL-10. (c) Diameter analysis of electrospun fibers. (d) Fluorographs of the outer grafted or inner encapsulated IL-10.

fibroblasts cultured in conditioned medium of monocytes/treated macrophages were performed by the methods as above mentioned (n = 3). The migration of the fibroblasts cultured in the conditioned medium of monocytes/macrophages was investigated with the methods as above mentioned (n = 3). The expression of scar related genes at both transcriptional and translational levels was detected by quantitative real-time PCR and western blot analysis, as described above (n = 3).

2.16. Wound healing model establishment and general observation

Full-thickness excisional wounds of 1.5 cm × 1.5 cm were made on the back of C57BL/6 mice. All institutional and national guidelines for the care and use of laboratory animals were followed. The wounds were covered with PLA-microsol electrospun membranes or PLA-microsol electrospun membranes with m-IL-10 both loaded inside and coated on the surface. These 1.5 cm × 1.5 cm electrospun membranes have the same thickness and weighed 8.36 mg. The wounds with no dressing were observed as the control (n = 3). The wound area was examined and

analyzed by Image J software every three days. Scar areas of PF group and PF-IL-10 group were compared with the control group on day 15.

2.17. Histological evaluation

On day 3 after operation, 3 mice of each group were examined by H&E staining and CD45 staining for inflammatory reaction assessment; and examined by F4/80 staining and CD163 staining for macrophages infiltration analysis (n = 3). Briefly, for H&E staining, the sections were fixed and stained nuclei with hematoxylin, stained cytoplasm with eosin. For IHC staining, the endogenous peroxidase of sections was inactivated by incubation with 3% of H_2O_2 for 10 min. Then the sections were incubated with 1:100 diluted antibodies, including CD45, F4/80, and CD163 at 4 °C overnight. Images were photographed under bright field microscope (Olympus, Tokyo, Japan). Image J software was used for statistical analysis of area positive-stained. On day 15, each scar tissue was fixed in 4% of neutral buffered formaldehyde, dehydrated, embedded in paraffin, and cut into 4-mm sections, which were
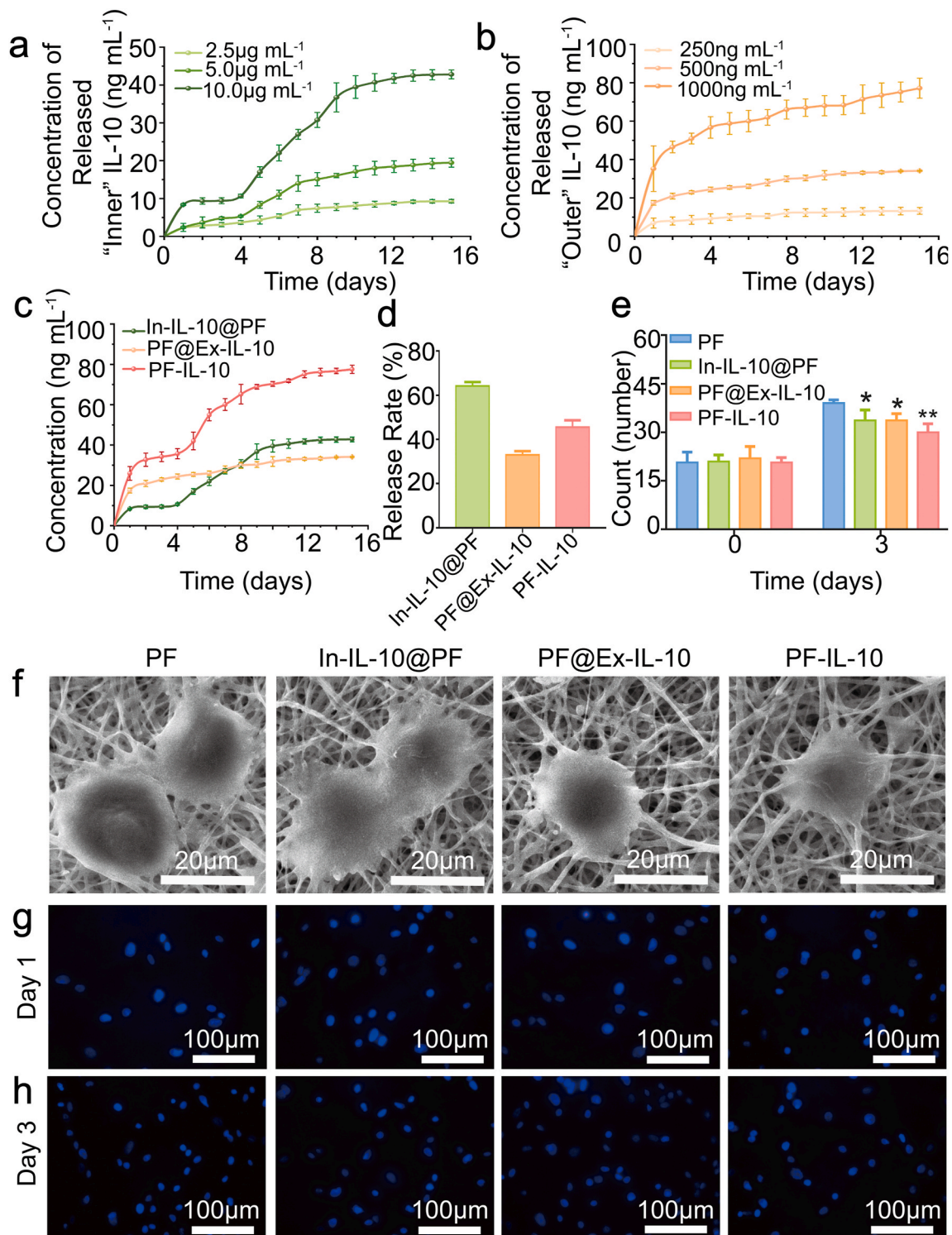
Fig. 3. Characterization of the electrospun membranes. (a, b) Release curves of "Inner" and "Outer" IL-10 of different amounts. (c, d) Release curves and rates of IL-10 from fibers. (e) Analysis of adherent cells quantity on day 1 and day 3. (f) SEM micrographs of adhesive cells. (g, h) Nuclear fluorescence staining of living cells on day 1 and day 3. *P < 0.05; **P < 0.01.

conducted with H&E, Masson trichrome, and IHC staining to observe the microscopic features of scar tissue with the methods as above mentioned (n = 3). Antibodies against Col I (1:100; Servicebio, Wuhan, China), Col III (1:100; Servicebio, Wuhan, China), MMP1 (1:100; Servicebio, Wuhan, China), TIMP1 (1:100; Servicebio, Wuhan, China), α-SMA (1:100; Servicebio, Wuhan, China), and VEGF (1:100; Servicebio, Wuhan, China) were used to access ECM deposition and angiogenesis.

2.18. Statistical analysis

Data are representative of three or more independent experiments. Statistical differences were determined by One-way ANOVA followed by Tukey's multiple comparison test. Results were expressed as mean ± standard deviation (SD). The differences were regarded as statistically significant with *P < 0.05, **P < 0.01, and ***P < 0.001.
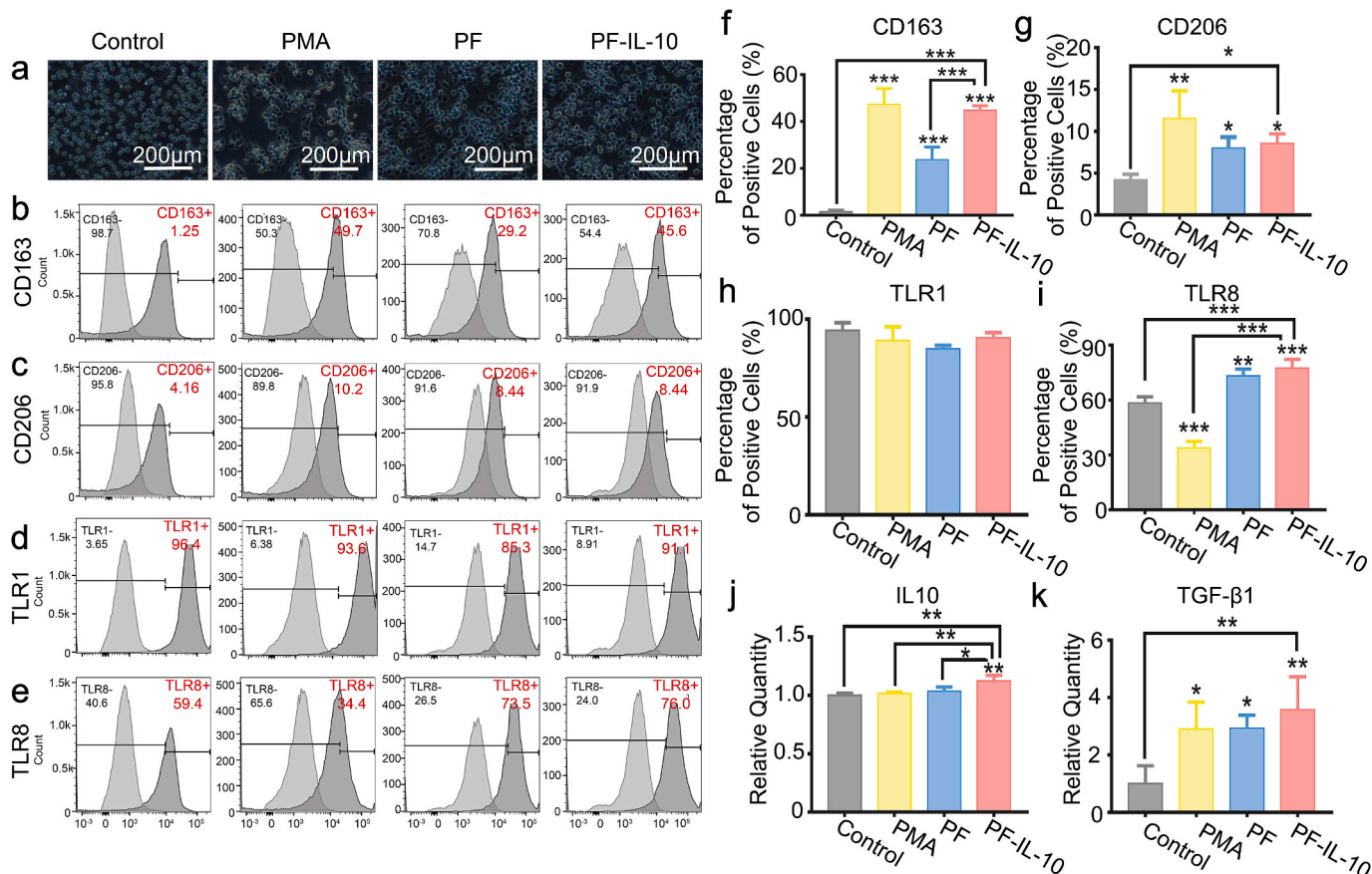
Fig. 4. Characterization of the stimulated macrophages. (a) Morphology of monocytes/stimulated macrophages. (b–e) Flow cytometry analysis of CD163, CD206, TLR1, and TLR8 expression. (f–i) Statistical analysis of CD163, CD206, TLR1, and TLR8 expression. (j, k) Evaluation of IL-10 and TGF-β1 secretion. *P < 0.05; **P < 0.01; ***P < 0.001.

3. Results and discussion

3.1. IL-10 concentration gradient effect on macrophage and fibroblast

In order to evaluate the range of effective IL-10 concentration, we used different concentrations of IL-10 (0 ng/mL, 10 ng/mL, 50 ng/mL, 100 ng/mL, 200 ng/mL, and 500 ng/mL) to perform *in vivo* and *in vitro* experiments on macrophages and fibroblasts. The number of inflammatory cells and "M2" macrophages in the local wound directly determines the degree of inflammatory response during the inflammatory phase and the quantity of pro-regenerative cytokines during the proliferation phase. As the concentration of IL-10 increased, the number of inflammatory cells decreased significantly (Figs. S3a, b, q). The total amount of local macrophages and the quantity of M2 macrophages were also significantly reduced when the IL-10 concentration was greater than 200 ng/mL (Figs. S3c and d, r, s, t). However, when the IL-10 concentration was lower than 200 ng/mL, there was no statistical difference between the experimental groups and the control group. This showed that when the *in vivo* concentration of IL-10 was between 50 and 100 ng/mL, it effectively inhibited the recruitment of neutrophils, while having no significant effect on the quantity of local polarized M2 macrophages. Furthermore, the *in vitro* proliferation experiment showed that when the IL-10 of concentration greater than 50 ng/mL exhibited a concentration-dependent inhibitory effect on the proliferation of fibroblasts (Fig. S3g). However, the IL-10 of 500 ng/mL showed cell damage potential (Figs. S3e, f, h). Therefore, the concentration of IL-10 acting on fibroblasts *in vivo* was preferably 100–200 ng/mL. After determining the IL-10 concentration of local wound skin tissue fluid (Fig. S3u) and the corresponding concentration of the *in vitro* release buffer (Fig. S3v-x),

we found that the IL-10 concentration of the local wound skin tissue fluid, which was released by the fibrous membrane, was about 1.91 times that of the *in vitro* release buffer. Considering the effective concentration range of IL-10 and the release behavior of electrospun fiber *in vitro* (Fig. S3i-p, Fig. 3a–c), the fiber loaded with 10 μg/mL of IL-10-HA-sol inside and grafted with 500 ng/mL of IL-10 outside maybe effective and was assigned as "PF-IL-10". We further performed the follow-up experiments to test this hypothesis.

3.2. Characteristics of "inner-outer" IL-10-loaded electrospun fiber

Here, we constructed an "Inner-Outer" IL-10-loaded PLA electrospun scaffold, as shown in Fig. 1a. In order to understand the performance of PF-IL-10 in depth, other fibers (PF, In-IL-10@PF, and PF@Ex-IL-10) were compared. From SEM images, the fibers of all the four groups were uniform, smooth and randomly oriented (Fig. 2a). The diameters of HA core in PF group and PF@Ex-IL-10 group were smaller than that of HA-IL-10 core in both In-IL-10@PF and PF-IL-10 groups (Fig. 2b). In order to quantify the difference of fiber diameter, 100 fibers in the TEM images were randomly selected from each group (Fig. 2c). The surface coated IL-10 made no contribution to overall diameter of fiber, while the inner diameter was significantly increased with the IL-10 encapsulated in the HA nanoparticle. To visualize the IL-10 distribution, IL-10 was labeled with FITC. Through microsol electrospinning technology and plasma surface treatment procedure [24,25], IL-10 was respectively loaded in the core of electrospun fiber and grafted on the fiber (Fig. 2d).

IL-10 is an anti-inflammatory and anti-fibrotic factor [26]. However, the influence of IL-10 concentration on its biological effects cannot be ignored, especially in consideration of different phases for the skin
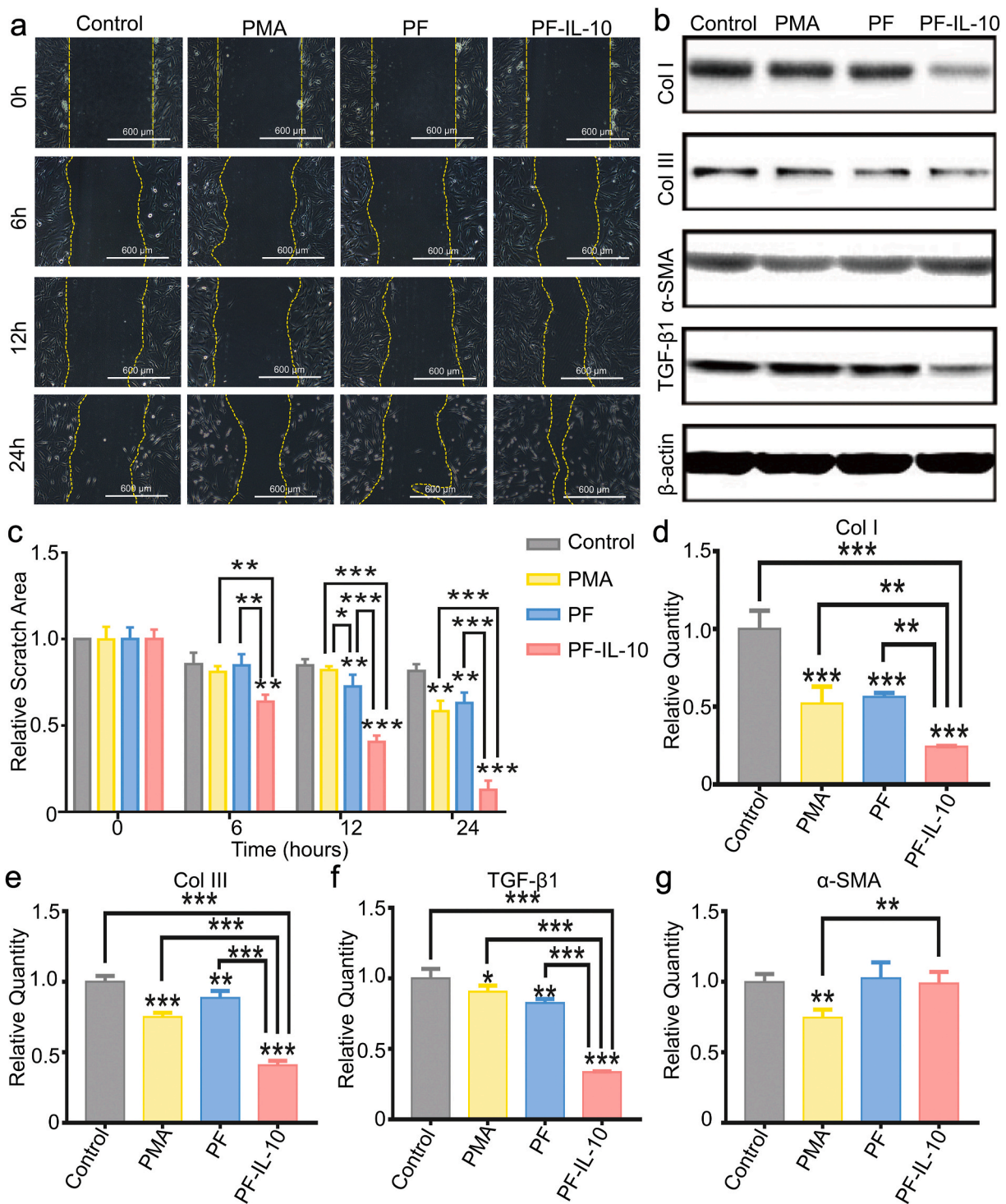
Fig. 5. The effect of stimulated macrophages on wound healing *in vitro*. (a, c) Morphological and quantitative analysis of fibroblasts migration area. (b) Western blot analysis of Col I, Col III, α-SMA, and TGF-β1. (d–g) Quantitative real-time PCR analysis of Col I, Col III, TGF-β1 and α-SMA. *P < 0.05; **P < 0.01; ***P < 0.001.

regeneration. The high concentration of IL-10 in the inflammatory phase will largely inhibit the recruitment of macrophages and subsequently affect the amount of macrophages secreted cytokines [27]. While the inhibitory effect of IL-10 on fibroblast proliferation in proliferative phase depends on a higher effective concentration [8,28,29]. Therefore, how to keep IL-10 at a relative low level during the inflammatory phase and maintain it at a higher level during the proliferative phase is a critical issue. As shown in Fig. 3a and b, the higher the concentration of IL-10 loaded inside, the more obvious delayed burst release is observed;

and the greater the amount of outside loaded cytokines, the more proteins released per unit time. Considering the release characteristics of "Inner" and "Outer" loaded IL-10, PF-IL-10 with IL-10 loaded both inside and outside was developed. Specifically, we loaded 10 μg/mL of IL-10 inside the fiber, and treated it with plasma procedure. After that, the plasma treated "Inner" IL-10 loaded scaffolds were immersed into 500 ng/mL of IL-10 solution for 24 h to construct the PF-IL-10. As a result, by detecting the release behavior of PF-IL-10, about 42.0 ng/mL of IL-10 was released in the first 5 days; and at a second higher burst release
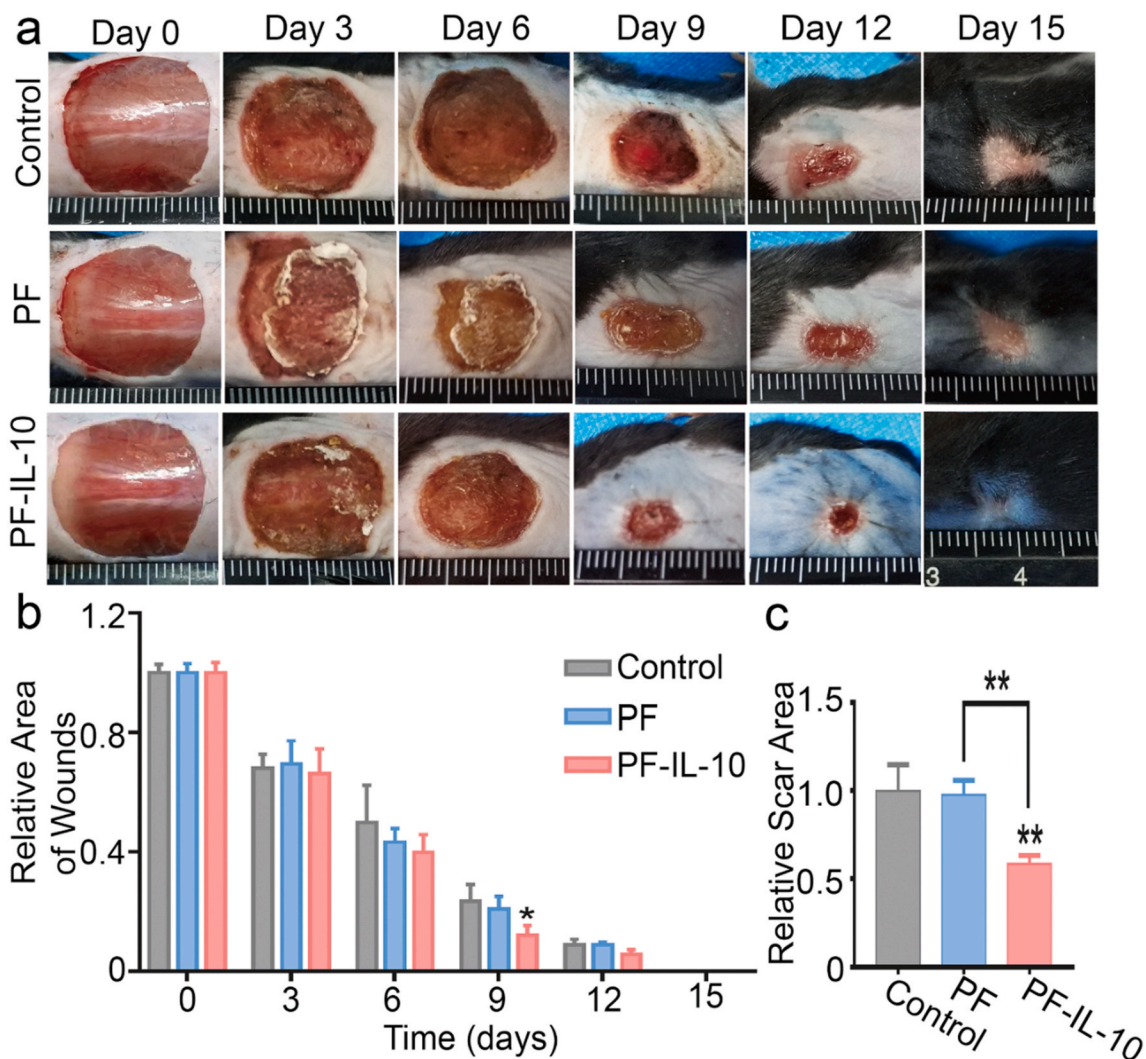
Fig. 6. *In vivo* therapeutic efficacy of PF-IL-10. (a) PF-IL-10 promotes wound healing *in vivo*. (b, c) Statistical analysis of the healing of skin defect and scar area. *P < 0.05, **P < 0.01.

initialed at day 5, about 35.5 ng/mL released between day 5 to day 15, the total cumulative concentration reaching 77.5 ng/mL on day 15 (n = 3) (Fig. 3c). In consideration of the concentration relation of the *in vivo* tissue fluid and *in vitro* release buffer, the temporal characteristics of release behavior was in close coordination with the process of wound healing. The proportion of the amount of IL-10 released from PF-IL-10 for 15 days was about 45.56% (n = 3) (Fig. 3d).

Direct contacting with tissue cells, an ideal biomaterial cannot only ensure the pharmacological effect of the drug, but also provide attachment for cell proliferation and migration without causing local inflammation and substantial damage [30]. After seeding fibroblast cells on the electrospun membranes, they adhered strongly to the surface of fibers and stretched very well, presenting a good appearance after 3 days (Fig. 3f). A significant increase in the number of fibroblasts was observed after 3 days' culture (Fig. 3g and h). These results indicated that the membranes of all the four groups have good biological compatibility. Compared with the PF group without IL-10 loaded, electrospun fiber loaded with IL-10 slowed down the growth of cells significantly (n = 6) (Fig. 3e).

3.3. Biological effect of "inner-outer" IL-10-loaded electrospun fiber on fibroblasts

Buffers of PF and PF-IL-10, which contained all the substances

released by the biomaterials, were collected on day 15. As shown in Fig. S4a, the density of fibroblasts cultured with PF-IL-10 releasing buffer was lower than that of the control group and PF group. Detected by a CCK-8 assay (Fig. S4b), the inhibiting effect of PF-IL-10 on fibroblast proliferation was significant compared with the other two groups on day 2 and day 3 (n = 6). Since PF components showed no effect on cell proliferation, apoptosis and membrane disruption, PF was proved to be an ideal carrier for IL-10 with low toxicity, good biodegradability and high biocompatibility (Figs. S4c–e).

Excessive scar formation is a common derailed regeneration outcome and is closely related to over proliferation of fibroblasts and excessive ECM deposition [31]. Col I and Col III are two important components of ECM. After culturing fibroblasts with releasing buffer of PF-IL-10 collected on day 15, the expression of Col I and Col III was significantly reduced at both transcription and translation levels (Figs. S5a–c). Although PF did not show the effect on Col I deposition, it significantly suppressed the production of Col III, which may be due to the biological effects caused by material degradation products [32]. The expression of alpha-smooth muscle actin (α-SMA), an established marker of myofibroblasts [33], was found to be reduced in PF-IL-10 group at transcription level (Fig. S5d). There was no statistically difference on the expression of TGF-β1 and the migration rate among different groups (Figs. S5e–g).
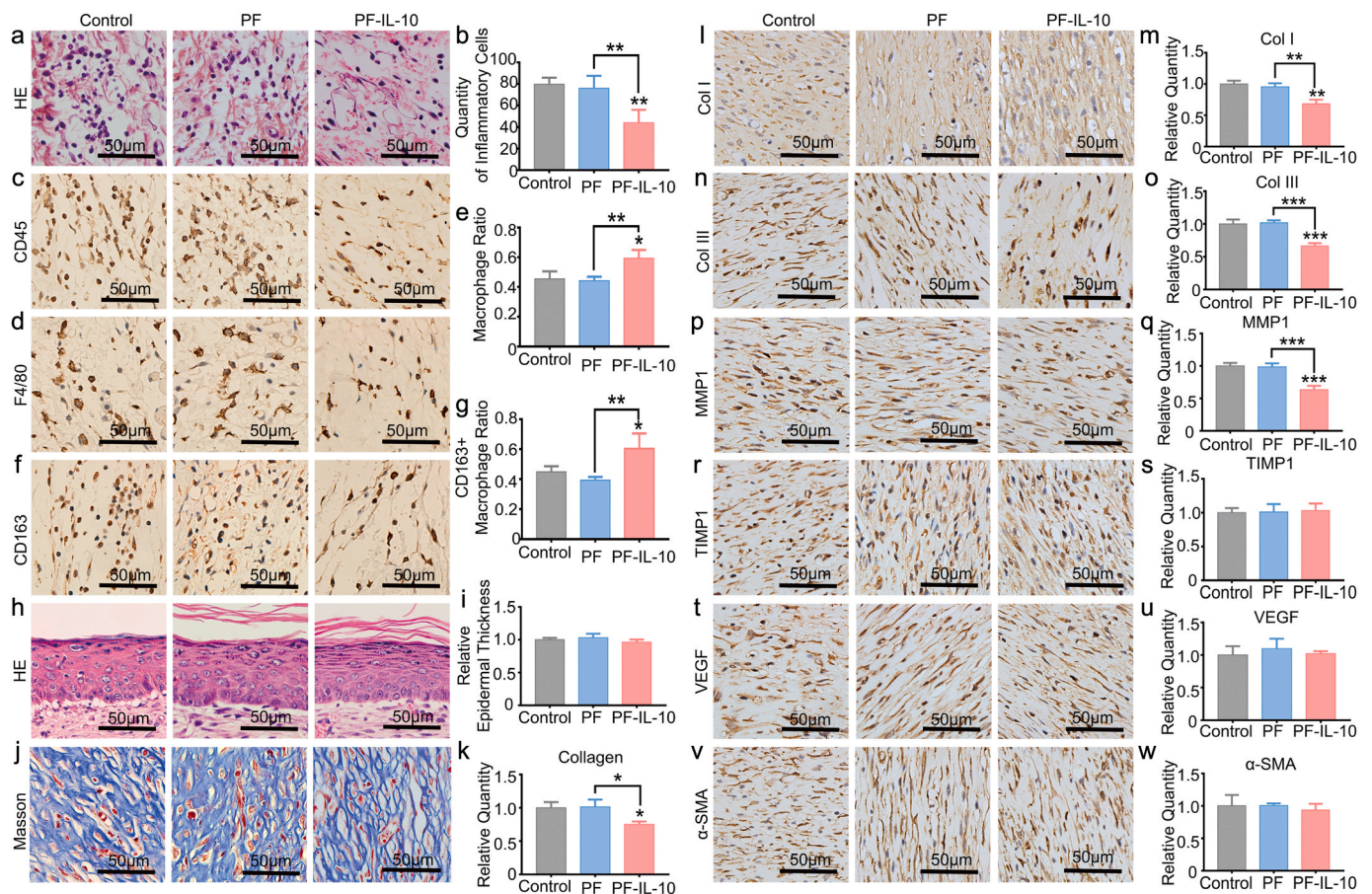
Fig. 7. Histological analysis in vivo. (a) H&E staining. (c) CD 45 IHC staining of leukocytes on day 3. (d, f) IHC staining of macrophages and CD163 positive macrophages on day 3. (b, e, g) Statistical analysis of inflammatory cells, macrophages, and CD163 positive macropahges on day 3. (h, i) H&E staining and epidermal thickness analysis on day 15. (j, k) Masson staining and statistical analysis of dermal collagen deposition on day 15. (l–w) IHC staining and statistical analysis of Col I, Col III, MMP1, TIMP1, VEGF, and α-SMA on day 15. *P < 0.05; **P < 0.01; ***P < 0.001.

3.4. Biological effect of "inner-outer" IL-10-loaded electrospun fiber stimulated macrophages

Macrophages are the most important immunoregulatory cells in the process of wound healing [34]. It has been clear that the macrophages can adopt its function and phenotype in response to microenvironment [35]. Therefore, programmatically regulating macrophage functions via modulating the microenvironment so as to coordinate with the wound healing process is the key to successful scarless wound healing.

In order to investigate the polarization effect of PF and PF-IL-10 on macrophages, we collected the releasing buffers of PF and PF-IL-10 on day 3 and examined the changes on cell morphology (Fig. 4a) and surface markers in vitro (Fig. 4b–e). Among the membrane proteins of the TLR family, the association of TLR1/TLR2 is essential for recognizing bacterial lipoproteins and lipopeptides [36]. The expression of TLR8 is predominantly engaged in evoking a dominant proinflammatory cytokine profile [37]. As shown in Fig. 4h, TLR1 expression was not affected by PF and PF-IL-10 (Fig. 4d, h). Compared with unstimulated THP-1, the expression of TLR8 in PMA-stimulated THP-1 cells decreased significantly (Fig. 4e, i). PF and PF-IL-10 stimulated macrophages with high expression of CD163 and CD206 (Fig. 4b, c, f, g) showed the characteristics of M2 macrophages. With IL-10 released by electrospun fibers as control, the additional IL-10 was observed to be secreted by the macrophages. PF-IL-10-stimulated macrophage secreted more IL-10 (Fig. 4j). The concentration of TGF-β1 in PF-IL-10 group reached 3.6 times as that of the control group (n = 6) (Fig. 4k). Overall, PF-IL-10-stimulated macrophage was activated to exert an immuno-modulatory role of "M2c" with high expression of CD163, CD206, TLR1,

and TLR8, and hypersecretion of IL-10 and TGF-β1 [18].

To further evaluate the stimulated macrophages/monocytes-mediated regeneration effect in vitro (Fig. S6), fibroblasts were cultured with the conditioned medium of THP-1, PMA-stimulated THP-1, PF-stimulated macrophage, and PF-IL-10-stimulated macrophage, respectively (n = 3). The proliferation of cells was inhibited in the PMA, PF, and PF-IL-10 groups (Figs. S6a and c). Among the three groups, conditioned medium of THP-1 stimulated by PMA had the strongest proliferation inhibitory and cytotoxic effect on cells (Figs. S6b, e, f), which was consistent with previous discovery that the increase of lysosomal numbers, the release of superoxide anions (O₂⁻) and prostaglandin E2 (PGE2), the enhancement of phospholipase A2 (PLA2) activity and the upregulation of protein kinase C (PKC) isoenzymes of PMA-stimuted THP-1 contributed to the cell death [38,39]. Also due to the cytokines secreted by PMA stimulated THP-1, the number of round fibroblasts increased after 24 h culture (Figs. S6a and d).

Different from the effect of the releasing buffer of PF-IL-10 on fibroblasts, the secretions of PF-IL-10 stimulated macrophages showed a strong effect on fibroblast migration (Fig. 5a, c). After 24 h of culture, the relative scratch area of PF-IL-10 was only 15.6% of that of the control group (n = 3). Moreover, the cytokines secreted by PF-IL-10-stimulated macrophages also significantly inhibited the expression of scar-related proteins at both transcription and translation levels. The expression of TGF-β1, Col I, and Col III in PF-IL-10 group dropped significantly to 33.6%, 24.2%, and 40.9% of that of the control group, respectively (n = 3) (Fig. 5d–f). Western blot analysis further confirmed the anti-scar effect of PF-IL-10-stimulated macrophage (Fig. 5b). Although with no effect on the expression of α-SMA (Fig. 5g), PF-

Fig. 8. Scheme of mechanism of the programmable immune activation in skin regeneration using "Inner-Outer" IL-10-loaded electrospun fibers.

stimulated macrophage also inhibited fibrosis by suppressing the expression of Col I, Col III, and TGF-β1 at the transcription level (Fig. 5d–f), showing a synergistic effect with PF-IL-10-stimulated macrophage.

3.5. In vivo effect of "inner-outer" IL-10-loaded electrospun fiber on wound healing

To further investigate the *in vivo* effect of PF-IL-10, we established a full-thickness cutaneous wound model on the dorsal skin of C57BL/6 mice [40]. As shown in Fig. 6a, the non-healing area treated with 1.5 cm × 1.5 cm of PF-IL-10 electrospun membrane of the same thickness was much smaller than that of both the control and PF groups after day 9 (Fig. 6b). On day 15, all wounds have closed, and scar areas without hair follicle growth can be seen. The treatment of PF-IL-10 mats significantly reduced the scar area by nearly 52.2% (n = 3) (Fig. 6c). Despite the procoagulant effect of the biological membrane, the scar area of PF group showed no difference with that of the control group.

Driven by chemokines in the local extracellular milieu, the amount of wound associated macrophages increases until day 2 and then remain stable until around day 5 [41,42]. From Fig. 7a–c, the quantity of

inflammatory cells on day 3 was largely decreased in PF-IL-10 group, which is due to the potent inhibiting effect of low concentration IL-10 on inflammatory cell recruitment. Associated with reduced infiltration of immune cells, the ratio of macrophages recruited increased (Fig. 7d and e), which suggested that the low concentration of IL-10 released by the scaffold had a stronger inhibition effect on the infiltration of neutrophils other than macrophages. In addition, with a higher ratio of CD163 positive macrophage, PF-IL-10 was shown to be able to promote "M2" macrophage polarization (Fig. 7f and g). Although the thickness of newly formed epidermis showed no difference with that of the control group (Fig. 7h and i), collagenous fibers of the skin were less-dense and less-pronounced in the PF-IL-10 group (Fig. 7j and k). The positive expression of Col I and Col III was also significantly decreased to 66.4% and 60.1% of the control group in the wounds treated with PF-IL-10 mats, which histologically demonstrated the anti-scar effect of PF-IL-10 scaffold (Fig. 7l–o). With decreased amount of ECM deposition, the expression of MMP1, a member of the family of matrix metal-loproteinase, was down-regulated in PF-IL-10 group; while whose expression in PF group did not change significantly (Fig. 7p, q). This result may be related to the feedback regulation of MMP1 on excessive collagen deposition. However, the expression of TIMP1, VEGF, and

α-SMA did not change in response to the increased concentration of IL-10 (Fig. 7r–w).

4. Conclusion

Overall, an "Inner-Outer" IL-10-loaded electrospun fiber with cascade behavior was developed to programmably activate immune response (Fig. 8). The initial burst release kept IL-10 at a lower concentration for the first 5 days, inhibiting excessive inflammatory response. The subsequent burst maintained the local IL-10 at a higher concentration in the proliferative phase, which not only maintained the polarization state of the anti-fibrotic macrophage "M2c", but also effectively inhibited dermal fibroblast over proliferation, thereby inhibiting excessive ECM deposition. The "Inner-Outer" IL-10-loaded electrospun fiber with cascade release behavior perfectly cooperated with the sequential wound healing process and programmatically activate the phased immune reactions that determine the outcome of tissue repair, thereby achieving scarless skin regeneration. Further, in view of the critical role of cytokine mediated immune response in sequential tissue regeneration process, the internal and external cytokine-loaded biomaterials regulation provides new insights for programmable tissue reparation and shows broad prospects in the field of damaged organ reconstruction.

CRediT authorship contribution statement

Lu Chen: conducted experiments, data Formal analysis, and . **Liucheng Zhang:** performed in vitro experiments. **Hongbo Zhang:** design materials experiments. **Xiaoming Sun:** performed experiments on materials and support the project with funding. **Dan Liu:** performed in vivo experiments. **Jianming Zhang:** supervised in vitro and in vivo experiments. **Yuguang Zhang:** supervised the project, and support the project with funding. **Liying Cheng:** support the project with funding. **Hélder A. Santos:** conceived the research, supervised the project, and support the project with funding. **Wenguo Cui:** conceived the research, supervised the project, and support the project with funding.

Declaration of competing interest

The authors declare that they have no known competing financial interests or personal relationships that could have appeared to influence the work reported in this paper.

Appendix A. Supplementary data

Supplementary data to this article can be found online at https://doi.org/10.1016/j.bioactmat.2021.02.022.

References

[1] V. Gabriel, Hypertrophic scar, Phys. Med. Rehabil. Clin 22 (2011) 301–310.

[2] S.A. Eming, T.A. Wynn, P. Martin, Inflammation and Metabolism in Tissue Repair and Regeneration, Science 356 (2017) 1026–1030.

[3] R. Ogawa, Recent advances in scar biology, Int. J. Mol. Sci. 19 (6) (2018) 1749.

[4] H. Sorg, D.J. Tilkorn, S. Hager, J. Hauser, U. Mirastschijski, Skin wound healing: an update on the current knowledge and concepts, Eur. Surg. Res. 58 (2017) 81–94.

[5] B. Mahdavian Delavary, W.M. van der Veer, M. van Egmond, F.B. Niessen, R. H. Beelen, Macrophages in skin injury and repair, Immunobiology 216 (2011) 753–762.

[6] Y. Qian, Y. Shen, S. Deng, T. Liu, F. Qi, Z. Lu, L. Liu, N. Shao, J. Xie, F. Ding, R. Liu, Dual functional β-peptide polymer-modified resin beads for bacterial killing and endotoxin adsorption, BMC Materials 1 (2019) 5.

[7] R. Sabat, G. Grütz, K. Warszawska, S. Kirsch, E. Witte, K. Wolk, J. Geginat, Biology of interleukin-10 21, Cytokine Growth Factor Rev., 2010, pp. 331–344.

[8] W.H. Peranteau, L. Zhang, N. Muvarak, A.T. Badillo, A. Radu, P.W. Zoltick, K. W. Liechty, IL-10 overexpression decreases inflammatory mediators and promotes regenerative healing in an adult model of scar formation, J. Invest. Dermatol. 128 (2008) 1852–1860.

[9] S. Balaji, X. Wang, A. King, L.D. Le, S.S. Bhattacharya, C.M. Moles, M.J. Butte, V. A. de Jesus Perez, K.W. Liechty, T.N. Wight, T.M. Crombleholme, P.L. Bollyky, S. G. Keswani, Interleukin-10-mediated regenerative postnatal tissue repair is dependent on regulation of hyaluronan metabolism via fibroblast-specific STAT3 signaling, Faseb. J. 31 (2017) 868–881.

[10] M. Jung, Y. Ma, R.P. Iyer, K.Y. DeLeon-Pennell, A. Yabluchanskiy, M.R. Garrett, M. L. Lindsey, IL-10 improves cardiac remodeling after myocardial infarction by stimulating M2 macrophage polarization and fibroblast activation, Basic Res. Cardiol. 112 (2017) 33.

[11] E.B. Lurier, D. Dalton, W. Dampier, P. Raman, S. Nassiri, N.M. Ferraro, R. Rajagopalan, M. Sarmady, K.L. Spiller, Transcriptome analysis of IL-10-stimulated (M2c) macrophages by next-generation sequencing, Immunobiology 222 (2017) 847–856.

[12] L. Tang, L. Hang, C. Wang, H. Li, Q. Zhang, J. Bai, M2a and M2c macrophage subsets ameliorate inflammation and fibroproliferation in acute lung injury through interleukin 10 pathway, Shock 48 (2017) 119–129.

[13] A. Mantovani, A. Sica, S. Sozzani, P. Allavena, A. Vecchi, M. Locati, The chemokine system in diverse forms of macrophage activation and polarization, Trends Immunol. 25 (2004) 677–686.

[14] H. Kadavil, M. Zagho, A. Elzatahry, T. Altahtamouni, Sputtering of electrospun polymer-based nanofibers for biomedical applications: a perspective, Nanomaterials 9 (2019) 77.

[15] E. Pugliese, J.Q. Coentro, M. Raghunath, D.I. Zeugolis, Wound healing and scar wars, Adv. Drug Deliv. Rev. 129 (2018) 1–3.

[16] J.H. Shi, H. Guan, S. Shi, W.X. Cai, X.Z. Bai, X.L. Hu, X.B. Fang, J.Q. Liu, K. Tao, X. X. Zhu, C.W. Tang, D.H. Hu, Protection against TGF-β1-induced fibrosis effects of IL-10 on dermal fibroblasts and its potential therapeutics for the reduction of skin scarring, Arch. Dermatol. Res. 305 (2013) 341–352.

[17] W. Chen, X. Tian, W. He, J. Li, Y. Feng, G. Pan, Emerging functional materials based on chemically designed molecular recognition, BMC Materials 2 (2020) 1.

[18] X. Huang, Y. Li, M. Fu, H.B. Xin, Polarizing macrophages in vitro, Methods Mol. Biol. 1784 (2018) 119–126.

[19] W. Sun, Y. Jiang, F. He, Extraction and proteome analysis of liver tissue interstitial fluid, Methods Mol. Biol. 728 (2011) 247–257.

[20] D.J. Hellenbrand, K.A. Reichl, B.J. Travis, M.E. Filipp, A.S. Khalil, D.J. Pulito, A. V. Gavigan, E.R. Maginot, M.T. Arnold, A.G. Adler, W.L. Murphy, A.S. Hanna, Sustained interleukin-10 delivery reduces inflammation and improves motor function after spinal cord injury, J. Neuroinflammation 16 (2019) 93.

[21] J.M. Reinke, H. Sorg, Wound repair and regeneration, Eur. Surg. Res. 49 (2012) 35–43.

[22] A. Kasuya, Y. Tokura, Attempts to accelerate wound healing, J. Dermatol. Sci. 76 (2014) 169–172.

[23] N.X. Landén, D. Li, M. Ståhle, Transition from inflammation to proliferation: a critical step during wound healing, Cell. Mol. Life Sci. 73 (2016) 3861–3885.

[24] G. Xia, H. Zhang, R. Cheng, H. Wang, Z. Song, L. Deng, X. Huang, H.A. Santos, W. Cui, Localized controlled delivery of gemcitabine via microsol electrospun fibers to prevent pancreatic cancer recurrence, Adv Healthc Mater 7 (2018), e1800593.

[25] H. Shen, X. Hu, J. Bei, S. Wang, The immobilization of basic fibroblast growth factor on plasma-treated poly(lactide-co-glycolide), Biomaterials 29 (2008) 2388–2399.

[26] W. Ouyang, S. Rutz, N.K. Crellin, P.A. Valdez, S.G. Hymowitz, Regulation and functions of the IL-10 family of cytokines in inflammation and disease, Annu. Rev. Immunol. 29 (2011) 71–109.

[27] I. Kieran, A. Knock, J. Bush, K. So, A. Metcalfe, R. Hobson, T. Mason, S. O'Kane, M. Ferguson, Interleukin-10 reduces scar formation in both animal and human cutaneous wounds: results of two preclinical and phase II randomized control studies, Wound Repair Regen. 21 (2013) 428–436.

[28] L. Zhang, Y. Ding, G.Z. Rao, D. Miao, Effects of IL-10 and glucose on expression of OPG and RANKL in human periodontal ligament fibroblasts, Braz. J. Med. Biol. Res. 49 (2016) e4324.

[29] C.J. Bodaan, L.M. Wise, K.A. Wakelin, G.S. Stuart, N.C. Real, A.A. Mercer, C. B. Riley, C. Theoret, Short-term treatment of equine wounds with orf virus IL-10 and VEGF-E dampens inflammation and promotes repair processes without accelerating closure, Wound Repair Regen. 24 (2016) 966–980.

[30] A. Nair, L. Tang, Influence of scaffold design on host immune and stem cell responses, Semin. Immunol. 29 (2017) 62–71.

[31] J. Zhang, Y. Li, X. Bai, Y. Li, J. Shi, D. Hu, Recent advances in hypertrophic scar, Histol. Histopathol. 33 (2018) 27–39.

[32] X. Li, C. Chu, Y. Wei, C. Qi, J. Bai, C. Guo, F. Xue, P. Lin, P.K. Chu, In vitro degradation kinetics of pure PLA and Mg/PLA composite: effects of immersion temperature and compression stress, Acta Biomater. 48 (2017) 468–478.

[33] A.V. Shinde, C. Humeres, N.G. Frangogiannis, The role of α-smooth muscle actin in fibroblast-mediated matrix contraction and remodeling, Biochim. Biophys. Acta (BBA) - Mol. Basis Dis. 1863 (2017) 298–309.

[34] K.L. Spiller, T.J. Koh, Macrophage-based therapeutic strategies in regenerative medicine, Adv. Drug Deliv. Rev. 122 (2017) 74–83.

[35] M.N. Artyomov, A. Sergushichev, J.D. Schilling, Integrating Immunometabolism and Macrophage Diversity, Semin Immunol 28 (2016) 417–424.

[36] N. Morita, I. Yamai, K. Takahashi, Y. Kusumoto, T. Shibata, T. Kobayashi, M. I. Nonaka, I. Ichimonji, H. Takagi, K. Miyake, S.A. Takamura, C4b binding protein negatively regulates TLR1/2 response, Innate Immun. 23 (2017) 11–19.

[37] M. Beesu, H.P. Kokatla, S.A. David, Syntheses of human TLR8-specific small-molecule agonists, Methods Mol. Biol. 1494 (2017) 29–44.

[38] H. Schwende, E. Fitzke, P. Ambs, P. Dieter, Differences in the state of differentiation of THP-1 cells induced by phorbol ester and 1,25-dihydroxyvitamin D3, J. Leukoc. Biol. 59 (1996) 555–561.

[39] M.E. Lund, J. To, B.A. O'Brien, S. Donnelly, The choice of phorbol 12-myristate 13-acetate differentiation protocol influences the response of THP-1 macrophages to a pro-inflammatory stimulus, J. Immunol. Methods 430 (2016) 64–70.

[40] Y. Li, W. Zhang, J. Gao, J. Liu, H. Wang, J. Li, X. Yang, T. He, H. Guan, Z. Zheng, S. Han, M. Dong, J. Han, J. Shi, D. Hu, Adipose tissue-derived stem cells suppress hypertrophic scar fibrosis via the p38/MAPK signaling pathway, Stem Cell Res. Ther. 7 (2016) 102.

[41] S.Y. Kim, M.G. Nair, Macrophages in wound healing: activation and plasticity, Immunol. Cell Biol. 97 (2019) 258–267.

[42] R.J. Snyder, J. Lantis, R.S. Kirsner, V. Shah, M. Molyneaux, M.J. Carter, Macrophages: a review of their role in wound healing and their therapeutic use, Wound Repair Regen. 24 (2016) 613–629.